

Glueball mass from RGZ-inspired infrared gluodynamics: a Euclidean Bethe–Salpeter approach

Rodrigo Carmo Terin^{1,*}

¹*King Juan Carlos University, Faculty of Experimental Sciences and Technology,
Department of Applied Physics, Av. del Alcalde de Móstoles, 28933, Madrid, Spain*

We formulate and solve a Euclidean Bethe–Salpeter equation (BSE) for the lightest 0^{++} glueball in pure Yang–Mills (YM) theory, using the refined Gribov–Zwanziger (RGZ) gluon tree-level propagator as an infrared-complete input. In a minimal ladder truncation with an effective constant kernel strength g_C^2 and the dominant s -wave component, we extract scalar glueball masses in the range $M_{0^{++}} \simeq 1.7\text{--}2.3$ GeV for representative values of g_C^2 , with a preferred value $M_{0^{++}} \simeq 1.9$ GeV around $g_C^2 \simeq 0.54$. The result is consistent with RGZ correlator-based infrared moment analyses and with lattice expectations, providing a cross-check of RGZ-inspired infrared gluodynamics from a bound-state viewpoint.

I. INTRODUCTION

Understanding the emergence of a physical, colorless spectrum from nonabelian YM theory [1] remains an important problem in quantum chromodynamics (QCD). A paradigmatic manifestation of confinement is the expected existence of glueballs, i.e. bound states with purely gluonic valence content. Although lattice simulations provide robust evidence for a discrete glueball spectrum in pure gauge theories, connecting these results to continuum frameworks that remain analytically controllable in the infrared (IR) is still a highly nontrivial task.

In continuum formulations, a gauge choice is required, and the standard Faddeev–Popov (FP) [2] procedure is incomplete in the IR due to the presence of Gribov copies [3, 4]. In the Landau gauge, large-volume lattice simulations have long established a decoupling-type gluon propagator: the transverse propagator saturates to a finite nonzero value as $p^2 \rightarrow 0$ while violating reflection positivity [5–8]. This behavior strongly suggests that the relevant IR degrees of freedom are not particle-like gluons, and that physical information must be extracted from gauge-invariant composite operators.

A prominent continuum strategy to incorporate the Gribov problem while preserving locality and renormalizability is the GZ framework [9, 10], and its Refined version (RGZ), where dimension-two condensates introduce additional IR mass scales that bring YM correlators in quantitative agreement with lattice data in the Landau gauge over a broad momentum window [11, 12]. An especially powerful formulation of RGZ employs the gauge-invariant transverse field A_μ^h , which enables one to retain an exact nilpotent BRST symmetry (in particular in linear covariant gauges), thereby ensuring a controlled renormalization of gauge-invariant composite operators and the associated Ward/Nielsen identities [13–15]. The resulting RGZ gluon propagator is IR-finite and typically exhibits complex conjugate poles, a concise analytic imprint of positivity violation and confinement.

A complementary continuum route, conceptually closer to lattice gauge fixing, is based on lifting the Gribov degeneracy by averaging over Gribov copies with a tunable weight in the Landau gauge. This was proposed by J. Serreau and M. Tissier and further work collaborators developed in covariant extensions and replica/superspace formulations [16–18]. In this approach, a replica nonlinear sigma-model sector induces a radiatively generated screening mass for the gluon through a phenomenon akin to symmetry restoration in the two-dimensional nonlinear sigma model, yielding an IR-safe perturbative description in a finite domain of renormalized parameters (without an IR Landau pole at one loop) [18]. More recently, our unified Landau-gauge fixing has been proposed that continuously interpolates between the Serreau–Tissier (ST) copy-averaged formulation and the RGZ restriction to the first Gribov region, by combining copy averaging with a horizon suppression in a single local, BRST-invariant and power-counting renormalizable action [19]. This unification gives a controlled theory to investigate how IR YM correlators depend on the balance between soft copy lifting and hard horizon suppression.

Within RGZ, one can access glueball physics through gauge-invariant correlators. An influential example is the infrared moment problem (a Padé/Hausdorff moment strategy) applied to the two-point functions of glueball operators using RGZ-inspired IR gluodynamics, which yields estimates $m_{0^{++}} \sim 2$ GeV and the hierarchy $m_{0^{++}} < m_{2^{++}} < m_{0^{-+}}$ already at the lowest moment order [20]. This correlator-based route is particularly natural in Euclidean signature, where glueball masses are extracted from the long-distance decay of Euclidean correlators, as in lattice computations.

* rodrigo.carmo@urjc.es

Another standard continuum route to bound states is through the famous Bethe–Salpeter equations (BSEs) [21] and related functional methods (Dyson–Schwinger equations (DSEs) and the functional renormalization group (FRG)), which organize the resummation of two-particle reducible diagrams into an eigenvalue problem whose discrete solutions determine the spectrum [22–24]. In hadron physics, there has also been substantial progress on solving the BSE directly in Minkowski space using the Nakanishi integral representation (NIR) and connecting it to light-front dynamics via light-front projection, providing direct access to timelike observables and light-front wave functions for dressed constituents [25–28]. While these Minkowski/light-front developments are mainly targeted at quark bound states, they clarify formal aspects of relativistic bound-state dynamics and motivate systematic connections between four-dimensional and projected three-dimensional formulations.

Moreover, continuum approaches based on BSEs have also been applied to the glueball spectrum using functional methods. Early DSEs/BSEs studies of scalar and pseudoscalar glueballs can be found in Ref. [29], whereas more recent developments include fully covariant two-gluon BSEs with ghost contributions [30] and parameter-free truncations derived from three-particle-irreducible effective actions [31]. These studies consistently report scalar glueball masses in the range $M_{0^{++}} \sim 1.6\text{--}2.0$ GeV, furnishing an important benchmark for our RGZ-inspired BSE framework developed here.

Therefore, in this work we follow an explicitly Euclidean strategy based on glueballs in pure YM: we formulate and solve a Euclidean BSE for the lightest scalar glueball ($J^{PC} = 0^{++}$), using as nonperturbative input the RGZ gluon propagator obtained in the BRST-invariant A_μ^h formulation. The scalar channel is naturally interpolated by the gauge-invariant local operator $\mathcal{O}_{0^{++}} = \frac{1}{4}F_{\mu\nu}^a F_{\mu\nu}^a$. Our BSE is constructed as an eigenvalue equation for the corresponding two-gluon Bethe–Salpeter amplitude in the color-singlet channel, with a symmetry-preserving ladder kernel as a first controlled truncation. Because the entire analysis is performed in Euclidean signature, the complex conjugate pole structure of the RGZ gluon propagator does not obstruct the integral equation on the integration domain; rather, it encodes confinement at the level of elementary fields, while the physical spectrum emerges only in the gauge-invariant composite channel. Besides providing an independent bound-state perspective complementary to correlator/moment methods, this Euclidean BSE framework offers direct access to the glueball amplitude and a transparent way to analyze truncation dependence and IR-input uncertainties. In particular, we can confront our extracted 0^{++} mass with RGZ correlator-based estimates and with lattice expectations, thereby testing the internal consistency of RGZ-inspired IR gluodynamics as an effective description of the confining YM infrared sector.

The paper is organized as follows. Section II reviews the BRST-invariant RGZ framework in terms of A_μ^h and fixes our conventions. Section III discusses glueball operators and the scalar channel. Section IV derives the Euclidean BSE for the 0^{++} glueball and specifies the truncation. Section V details the numerical strategy and stability tests. Section VI presents results and compares them with RGZ correlator/moment approaches. We conclude with an outlook on improving the kernel and extending the analysis to other J^{PC} channels.

II. THE REFINED GRIBOV–ZWANZIGER FRAMEWORK IN THE BRST-INVARIANT FORMULATION

We consider pure YM theory formulated in four-dimensional Euclidean space and quantized in the Landau gauge,

$$\partial_\mu A_\mu^a = 0. \quad (1)$$

At low energies, the standard FP quantization is known to be incomplete due to the presence of Gribov copies, i.e. gauge-equivalent configurations that satisfy the same gauge condition [3, 4]. The RGZ approach gives an effective infrared completion of YM theory that incorporates these effects and at the same time preserving locality and renormalizability [9–11].

A particularly powerful formulation of the RGZ theory is attained by expressing the action in terms of the gauge-invariant transverse field A_μ^h [13, 14]. This field is defined as the gauge transform of A_μ that minimizes the functional

$$\int d^4x A_\mu^a A_\mu^a \quad (2)$$

along the gauge orbit, and it can be constructed order by order as a nonlocal but gauge-invariant functional of A_μ . By construction, A_μ^h is transverse,

$$\partial_\mu A_\mu^{h,a} = 0, \quad (3)$$

and invariant under infinitesimal gauge transformations. This formulation enables the RGZ action to be endowed with an exact nilpotent BRST symmetry, despite the presence of the Gribov horizon [13, 14]. This property is fundamental

in our present work, as it ensures that gauge-invariant composite operators admit a consistent renormalization and can be meaningfully employed as interpolating fields in bound-state equations.

The RGZ action can be then written schematically as

$$S_{\text{RGZ}} = S_{\text{YM}} + S_{\text{FP}} + S_{\text{horizon}} + S_{\text{cond}}, \quad (4)$$

where S_{YM} denotes the YM action, S_{FP} the standard FP gauge-fixing term in the Landau gauge, and S_{horizon} implements the restriction of the functional integral to the first Gribov region.

In the local formulation, the horizon term reads

$$\begin{aligned} S_{\text{horizon}} = & \int d^4x \left[\bar{\varphi}_\mu^{ac} \mathcal{M}^{ab}(A^h) \varphi_\mu^{bc} - \bar{\omega}_\mu^{ac} \mathcal{M}^{ab}(A^h) \omega_\mu^{bc} \right] \\ & - \gamma^2 g \int d^4x f^{abc} A_\mu^{h,a} (\varphi_\mu^{bc} + \bar{\varphi}_\mu^{bc}), \end{aligned} \quad (5)$$

in which $\mathcal{M}^{ab}(A^h) = -\partial_\mu D_\mu^{ab}(A^h)$ is the FP operator, $\{\varphi, \bar{\varphi}\}$ are bosonic auxiliary fields, $\{\omega, \bar{\omega}\}$ their fermionic counterparts, and γ is the Gribov parameter fixed self-consistently by the horizon condition following from the minimization of the vacuum energy [9, 10].

Nonperturbative effects beyond the horizon restriction are encoded through dimension-two condensates. Including their contribution leads to the RGZ action [11, 12],

$$S_{\text{cond}} = \frac{m^2}{2} \int d^4x A_\mu^{h,a} A_\mu^{h,a} - M^2 \int d^4x (\bar{\varphi}_\mu^{ab} \varphi_\mu^{ab} - \bar{\omega}_\mu^{ab} \omega_\mu^{ab}), \quad (6)$$

where m^2 and M^2 are dynamically generated mass scales associated with the condensates $\langle A_\mu^{h,a} A_\mu^{h,a} \rangle$ and $\langle \bar{\varphi} \varphi - \bar{\omega} \omega \rangle$, respectively.

Throughout this work, all quantities are defined in Euclidean space. No assumption of a fundamental Minkowski formulation of the RGZ theory is made. This is consistent with both the lattice formulation of YM theory and the intrinsically nonperturbative nature of the observables under consideration. In particular, this choice is deliberate, as glueball masses are Euclidean observables customarily extracted from the long-distance behavior of Euclidean correlation functions.

Nonetheless, the central nonperturbative ingredient in the present analysis is the gluon two-point function obtained from the RGZ framework. In the BRST-invariant formulation based on the transverse field A_μ^h , the gluon propagator is well defined, multiplicatively renormalizable, and directly comparable to lattice results in the Landau gauge. At tree level, the RGZ action yields the following transverse gluon propagator in four-dimensional Euclidean space-time [11, 12]:

$$D_{\mu\nu}^{ab}(p) = \delta^{ab} \left(\delta_{\mu\nu} - \frac{p_\mu p_\nu}{p^2} \right) \mathcal{D}(p^2), \quad (7)$$

with the scalar form factor

$$\mathcal{D}(p^2) = \frac{p^2 + M^2}{p^4 + (m^2 + M^2)p^2 + m^2 M^2 + 2g^2 N \gamma^4}. \quad (8)$$

Although obtained at tree level, this propagator effectively resums dominant infrared dynamics through the presence of the condensates and provides an accurate description of lattice data over a broad momentum range. The propagator (8) exhibits a decoupling-type infrared behavior, remaining finite at vanishing momentum,

$$\mathcal{D}(0) = \frac{M^2}{m^2 M^2 + 2g^2 N \gamma^4} \neq 0, \quad (9)$$

in qualitative and quantitative agreement with large-volume lattice simulations of YM theory in the Landau gauge [5, 6, 8].

A distinctive feature of the RGZ propagator is its analytic structure. The denominator of Eq. (8) is a quartic polynomial in p^2 , which generically factorizes into two complex conjugate poles,

$$p^2 = -m_\pm^2, \quad m_\pm^2 = \mu^2 \pm i\theta^2, \quad (10)$$

with $\mu^2, \theta^2 > 0$. As a consequence, the gluon propagator violates reflection positivity, a hallmark of confinement [5, 11, 32]. Such complex conjugate poles can be interpreted as an effective parametrization of infrared gluonic correlations

rather than physical asymptotic states, and they provide a controlled analytic encoding of confinement effects. Despite the absence of a standard Källén–Lehmann representation with a positive spectral density at the level of elementary fields, the RGZ framework allows one to consistently define and renormalize gauge-invariant composite operators, whose correlation functions possess a well-defined analytic structure suitable for the extraction of physical observables. In the present work, the propagator (7)–(8) is taken as nonperturbative infrared input for the bound-state analysis. The use of the RGZ gluon propagator thus provides a self-consistent and lattice-compatible starting point for the formulation of a Euclidean BSE describing glueball bound states.

III. GLUEBALL STATES AND GAUGE-INVARIANT COMPOSITE OPERATORS

Glueballs are color-singlet bound states generated by the self-interactions of YM fields. In a confining theory, they do not correspond to poles of elementary gluon propagators, but rather appear as isolated poles, or dominant exponential scales, in correlation functions of gauge-invariant composite operators. This notion of the physical spectrum is standard in confining gauge theories and underlies both lattice simulations and continuum approaches based on operator correlation functions.

In Euclidean space, consider a local, gauge-invariant operator $\mathcal{O}(x)$ carrying definite quantum numbers J^{PC} . Its two-point correlation function is defined as

$$\Pi(x - y) = \langle \mathcal{O}(x) \mathcal{O}(y) \rangle, \quad (11)$$

which is translation invariant and thus depends only on $z = x - y$. It admits the Fourier representation

$$\Pi(p) = \int d^4z e^{-ip \cdot z} \Pi(z). \quad (12)$$

If \mathcal{O} couples to a discrete lowest-lying state of mass M in the given channel, the Euclidean correlator at large Euclidean time separation behaves as

$$\int d^3x \Pi(\tau, x) \xrightarrow{\tau \rightarrow \infty} \mathcal{Z} e^{-M\tau}, \quad (13)$$

which is the standard lattice route to extracting glueball masses. Equivalently, in momentum space one expects (up to subtractions) a spectral representation of the form

$$\Pi(p^2) = \int_0^\infty ds \frac{\rho(s)}{s + p^2}, \quad \rho(s) \geq 0, \quad (14)$$

whenever \mathcal{O} is gauge invariant and the corresponding physical Hilbert space is positive. In practice, approximate representations or truncations of $\Pi(p^2)$ are often employed, provided they preserve a sensible spectral density in the physical channels.

In this work we focus on the lightest scalar glueball channel,

$$J^{PC} = 0^{++}. \quad (15)$$

The lowest-dimensional local gauge-invariant operator carrying these quantum numbers is

$$\mathcal{O}_{0^{++}}(x) = \frac{1}{4} F_{\mu\nu}^a(x) F_{\mu\nu}^a(x), \quad (16)$$

where the YM field-strength tensor is

$$F_{\mu\nu}^a = \partial_\mu A_\nu^a - \partial_\nu A_\mu^a + g f^{abc} A_\mu^b A_\nu^c. \quad (17)$$

The normalization factor $\frac{1}{4}$ in Eq. (16) is conventional and plays no role in the bound-state condition. Since $\mathcal{O}_{0^{++}}$ is gauge invariant, its correlator represents a physical observable. Within the BRST-invariant RGZ formulation based on the transverse field A_μ^h , this operator can be consistently renormalized, and its correlation functions can be computed in a controlled way. This point is essential, because the elementary gluon propagator in RGZ violates reflection positivity and typically exhibits complex conjugate poles; therefore, physical information must be extracted at the level of gauge-invariant composite operators rather than from elementary fields.

For the purposes of a BSE treatment, it is instructive to make explicit the leading “two-gluon” content of \mathcal{O}_{0++} . Expanding Eq. (17) in powers of the gauge field, we write

$$F_{\mu\nu}^a = F_{\mu\nu}^{a,(1)} + F_{\mu\nu}^{a,(2)}, \quad (18)$$

with

$$F_{\mu\nu}^{a,(1)} = \partial_\mu A_\nu^a - \partial_\nu A_\mu^a, \quad (19)$$

$$F_{\mu\nu}^{a,(2)} = g f^{abc} A_\mu^b A_\nu^c. \quad (20)$$

The scalar operator then decomposes as

$$\mathcal{O}_{0++} = \frac{1}{4} F_{\mu\nu}^{a,(1)} F_{\mu\nu}^{a,(1)} + \frac{1}{2} F_{\mu\nu}^{a,(1)} F_{\mu\nu}^{a,(2)} + \frac{1}{4} F_{\mu\nu}^{a,(2)} F_{\mu\nu}^{a,(2)}. \quad (21)$$

The first term is quadratic in A_μ^a and provides the minimal two-gluon component relevant for a BSE description. In momentum space one has

$$F_{\mu\nu}^{a,(1)}(p) = i(p_\mu A_\nu^a(p) - p_\nu A_\mu^a(p)), \quad (22)$$

leading to

$$\frac{1}{4} F_{\mu\nu}^{a,(1)}(p) F_{\mu\nu}^{a,(1)}(-p) = \frac{1}{2} A_\mu^a(p) \left(p^2 \delta_{\mu\nu} - p_\mu p_\nu \right) A_\nu^a(-p). \quad (23)$$

This expression explicitly shows that the scalar operator projects onto transverse gluonic modes, as expected in the Landau gauge and consistent with the tensor structure of the RGZ gluon propagator. The remaining terms in Eq. (21) are cubic and quartic in the gauge field and, from the viewpoint of a bound-state truncation, correspond to higher Fock components and interaction corrections. In a BSE framework, such contributions are systematically incorporated through the interaction kernel rather than being kept explicitly in the interpolating operator.

The color structure of \mathcal{O}_{0++} is the trivial singlet. At the level of the leading quadratic term (23), this corresponds to contracting two adjoint indices with δ^{ab} . Accordingly, the color-singlet projector for a two-gluon state reads

$$\mathcal{P}_1^{ab} = \frac{\delta^{ab}}{\sqrt{N^2 - 1}}, \quad (24)$$

up to normalization conventions. Parity and charge-conjugation quantum numbers follow from the transformation properties of $F_{\mu\nu}^a F_{\mu\nu}^a$. In Minkowski space one has $F_{\mu\nu}^a F^{\mu\nu} = 2(\mathbf{B}^2 - \mathbf{E}^2)$, which is even under both parity and charge conjugation. In Euclidean space, the operator remains a scalar under $O(4)$ rotations and assumes $P = +$ and $C = +$ from the fundamental Minkowski theory, thereby coupling to 0^{++} states.

There are two complementary continuum strategies to access the glueball spectrum:

- (i) Compute the correlator $\Pi(p^2)$ of a gauge-invariant operator, such as \mathcal{O}_{0++} , using an effective infrared description (here RGZ), and extract the mass from its spectral representation or from suitable moment or sum-rule techniques. This approach is particularly natural within RGZ, where analytic expressions for infrared YM correlators are available.
- (ii) Formulate a bound-state equation for an effective two-body amplitude $\Gamma(p; P)$, whose constituents are infrared gluonic degrees of freedom described by the RGZ propagator, and determine $P^2 = -M^2$ from the existence of nontrivial solutions.

In this work we follow route (ii), which gives direct access to the glueball Bethe–Salpeter amplitude and enables for a systematic analysis of truncation and kernel dependence, and at the same time remaining entirely within Euclidean signature. The fundamental observation justifying a BSE formulation is that, at leading order in a skeleton expansion, the two-point function of a bilinear gauge-invariant operator receives contributions that can be organized into two-particle reducible gluon ladders. Resumming these ladders leads to an eigenvalue problem whose homogeneous form is precisely a BSE. Operationally, we treat the scalar glueball as a two-gluon bound state in the color-singlet channel, with the RGZ gluon propagator as the constituent two-point function and with an interaction kernel that captures the dominant infrared gluonic exchanges. Although the RGZ gluon propagator contains complex conjugate poles, this does not obstruct the extraction of physical glueball masses. The bound-state condition and mass determination are formulated entirely in Euclidean space and anchored to gauge-invariant quantities, in close analogy with lattice calculations. The role of the RGZ propagator is to provide a realistic, infrared-saturated two-point input consistent with confinement-related positivity violation, whereas physical poles emerge only in composite, gauge-invariant channels.

With these points established, we now turn to the explicit formulation of the Euclidean BSE for the 0^{++} glueball.

IV. EUCLIDEAN BETHE–SALPETER EQUATION FOR THE SCALAR GLUEBALL

In this section we formulate a Euclidean BSE for the scalar glueball in the channel $J^{PC} = 0^{++}$, using the RGZ gluon propagator as nonperturbative input as previously mentioned. The construction follows standard bound-state techniques in continuum quantum field theory and is adapted here to the case of confined gluonic degrees of freedom in YM theory.

We start from the connected four-point Green function of gluon fields, projected onto the color-singlet channel,

$$G_{\mu\nu\rho\sigma}^{(4)}(x_1, x_2; x_3, x_4) = \langle A_\mu^a(x_1) A_\nu^a(x_2) A_\rho^b(x_3) A_\sigma^b(x_4) \rangle_{\text{conn}}, \quad (25)$$

where repeated color indices are summed over. In momentum space, and after amputation of external legs, this object defines the two-particle scattering kernel for gluonic correlations in the adjoint representation. If a bound state with total Euclidean momentum P exists in the corresponding channel, general field-theoretical arguments imply that the four-point function develops a pole of the form

$$G^{(4)} \sim \frac{\Gamma_{\mu\nu}(p; P) \bar{\Gamma}_{\rho\sigma}(q; P)}{P^2 + M^2} \quad \text{for } P^2 \rightarrow -M^2, \quad (26)$$

in which M is the bound-state mass and $\Gamma_{\mu\nu}(p; P)$ denotes the Bethe–Salpeter amplitude, that depends on the relative momentum p and the total momentum P . This pole structure follows from analyticity and completeness and does not rely on the existence of asymptotic gluon states, which are absent in a confining theory.

Resumming the two-particle reducible contributions in the s -channel leads to a homogeneous integral equation for the Bethe–Salpeter amplitude,

$$\Gamma_{\mu\nu}(p; P) = \int \frac{d^4 q}{(2\pi)^4} \mathcal{K}_{\mu\nu\rho\sigma}(p, q; P) D_{\rho\alpha}(q_+) D_{\sigma\beta}(q_-) \Gamma_{\alpha\beta}(q; P), \quad (27)$$

where $q_{\pm} = q \pm P/2$ and $D_{\mu\nu}$ is the RGZ gluon propagator introduced in Eqs. (7)–(8). The kernel $\mathcal{K}_{\mu\nu\rho\sigma}$ collects all two-particle irreducible interactions in the chosen truncation. In the present work we employ a symmetry-preserving ladder truncation, corresponding to the lowest-order skeleton expansion. This approximation captures the dominant infrared interactions responsible for binding, whereas keeping the analysis analytically transparent. Higher-order corrections, for instance crossed-ladder diagrams and explicit three- and four-gluon vertex dressings, are neglected at this stage and will be addressed in future refinements.

For the scalar glueball channel $J^{PC} = 0^{++}$, the Bethe–Salpeter amplitude can be decomposed in terms of transverse tensors consistent with Lorentz symmetry, parity, and charge conjugation. At leading order, only one independent scalar structure contributes, and we write

$$\Gamma_{\mu\nu}(p; P) = \left(\delta_{\mu\nu} - \frac{P_\mu P_\nu}{P^2} \right) \Phi(p; P), \quad (28)$$

in which $\Phi(p; P)$ is a scalar Bethe–Salpeter amplitude. Substituting the decomposition (28) into Eq. (27) and performing the tensor contractions yields a scalar integral equation of the form

$$\Phi(p; P) = \int \frac{d^4 q}{(2\pi)^4} \mathcal{K}(p, q; P) \mathcal{D}(q_+^2) \mathcal{D}(q_-^2) \Phi(q; P), \quad (29)$$

where $\mathcal{D}(p^2)$ is the scalar part of the RGZ gluon propagator and $\mathcal{K}(p, q; P)$ denotes an effective scalar kernel determined by the chosen truncation. Equation (29) constitutes a homogeneous eigenvalue problem. Nontrivial solutions exist only for discrete values of P^2 , and the lowest eigenvalue defines the mass of the lightest scalar glueball,

$$P^2 = -M_{0^{++}}^2. \quad (30)$$

A potential concern in the RGZ framework, however, is the presence of complex conjugate poles in the gluon propagator. Indeed, this feature does not invalidate the Bethe–Salpeter construction for several reasons:

- The BSE is formulated entirely in Euclidean space, where the RGZ propagator is analytic and free of singularities on the integration domain.
- The bound-state condition is imposed on a gauge-invariant composite amplitude and does not correspond to a pole of the elementary gluon propagator.

- Glueball masses are extracted from Euclidean correlation functions, in direct analogy with lattice simulations of YM theory.

The complex analytic structure of the RGZ propagator should therefore be interpreted as a manifestation of confinement at the level of elementary fields, whereas physical poles emerge only in composite, gauge-invariant channels.

With the Euclidean BSE established, we now turn to its numerical solution, renormalization procedure, and stability analysis.

V. NUMERICAL STRATEGY AND RENORMALIZATION

In this section we detail the numerical reduction of the Euclidean BSE derived in Sec. IV, and clarify the role of renormalization when the RGZ gluon propagator is employed as an infrared-complete effective input. All calculations are performed in Euclidean space. The total momentum P of the bound state satisfies the on-shell condition

$$P^2 = -M_{0^{++}}^2 < 0, \quad (31)$$

while p denotes the relative momentum. We introduce the shifted loop momenta

$$q_{\pm} = q \pm \frac{P}{2}. \quad (32)$$

Owing to $O(4)$ covariance, the scalar Bethe–Salpeter amplitude depends only on the invariants

$$p^2, \quad z_p := \frac{p \cdot P}{\sqrt{p^2 P^2}}, \quad P^2, \quad (33)$$

and analogously for q . We choose a frame where the total momentum points along the Euclidean 4-axis,

$$P_{\mu} = (0, 0, 0, \sqrt{P^2}), \quad (34)$$

so that $z_p \in [-1, 1]$ and

$$q_{\pm}^2 = q^2 + \frac{P^2}{4} \pm \sqrt{q^2 P^2} z_q. \quad (35)$$

All integration variables remain real for $P^2 > 0$ in this convention. Although the RGZ gluon propagator $\mathcal{D}(k^2)$ possesses complex conjugate poles in the complex k^2 plane, the Euclidean integration domain never crosses these singularities.

Using the tensor decomposition discussed in Sec. IV, the scalar BSE can be written as

$$\Phi(p^2, z_p; P^2) = \int \frac{d^4 q}{(2\pi)^4} \mathcal{K}(p, q; P) \mathcal{D}(q_+^2) \mathcal{D}(q_-^2) \Phi(q^2, z_q; P^2), \quad (36)$$

where \mathcal{K} denotes the effective scalar kernel resulting from color and tensor contractions. For numerical purposes it is convenient to cast the BSE into an eigenvalue problem by introducing a parameter $\lambda(P^2)$,

$$\Phi(p) = \lambda(P^2) \int \frac{d^4 q}{(2\pi)^4} \mathcal{K}(p, q; P) \mathcal{D}(q_+^2) \mathcal{D}(q_-^2) \Phi(q), \quad (37)$$

where $\Phi(p) \equiv \Phi(p^2, z_p; P^2)$. For a fixed kernel model and fixed RGZ parameters, the bound-state mass is obtained from the condition

$$\lambda_{\max}(P^2) = 1, \quad (38)$$

where $\lambda_{\max}(P^2)$ denotes the largest eigenvalue of the integral operator. In practice, $\lambda_{\max}(P^2)$ is monotonic for a wide class of ladder-type kernels, enabling for a stable one-dimensional root-finding procedure. This strategy is standard in functional approaches to bound states based on DSEs and BSEs [22, 23].

The angular dependence of the amplitude is expanded in Chebyshev polynomials,

$$\Phi(p^2, z_p; P^2) = \sum_{n=0}^{N_z} \Phi_n(p^2; P^2) T_n(z_p), \quad (39)$$

with $T_n(z) = \cos(n \arccos z)$. The truncation order N_z is chosen such that the extracted mass is stable under increasing N_z . The four-dimensional integration measure is written as

$$\int \frac{d^4 q}{(2\pi)^4} = \frac{1}{(2\pi)^4} \int_0^\infty dq q^3 \int d\Omega_3, \quad (40)$$

with the angular dependence parameterized by z_q . For the radial integration we employ the mapping

$$q^2 = \Lambda^2 \frac{x}{1-x}, \quad x \in [0, 1), \quad (41)$$

which yields

$$q^3 dq = \frac{\Lambda^4}{2} \frac{x dx}{(1-x)^3}. \quad (42)$$

The scale Λ controls the transition between infrared and ultraviolet sampling and is varied to ensure numerical stability.

After discretization, Eq. (37) becomes a matrix eigenvalue problem,

$$\Phi = \lambda(P^2) \mathbf{M}(P^2) \Phi, \quad (43)$$

where $\mathbf{M}(P^2)$ encodes the kernel, propagators and quadrature weights. For each trial value of P^2 , the largest eigenvalue is computed using standard iterative methods. The homogeneous BSE determines the amplitude only up to an overall normalization. A physical normalization can be imposed through the canonical condition derived from the residue of the four-point function at the bound-state pole,

$$1 = \frac{d}{dP^2} \int \frac{d^4 q}{(2\pi)^4} \frac{d^4 k}{(2\pi)^4} \bar{\Gamma}(q; P) D(q_+) D(q_-) \Gamma(k; P) \Big|_{P^2 = -M^2}. \quad (44)$$

This normalization is essential for computing decay constants or transition form factors, but it is not required for the extraction of the bound-state mass itself.

A fundamental point of our present approach concerns renormalization. We do not renormalize the BSE in the perturbative FP sense, since we do not employ bare propagators or vertices. Instead, the RGZ gluon propagator is taken as a renormalized effective input, whose parameters (m^2, M^2, γ^4) are fixed by RGZ gap equations and/or lattice fits in a given renormalization scheme [11, 12]. Any multiplicative wave-function renormalization is already absorbed into these parameters.

The effective interaction strength entering the kernel is treated as a model parameter. Varying it within a controlled range provides an estimate of truncation uncertainties, in direct analogy with common practice in DSEs and BSEs studies. Ultraviolet stability is ensured by the $1/p^2$ falloff of the RGZ propagator at large momenta, and explicit cutoff dependence is monitored numerically.

It is worth emphasizing that the present strategy is conceptually close to the infrared moment problem approach of Ref. [20]. In that framework, glueball mass estimates display a residual dependence on the subtraction scale T , which is not a physical parameter and is fixed by an optimization criterion such as minimal sensitivity. In the present Euclidean BSE formulation, an analogous role is played by the effective kernel strength (and, to a lesser extent, numerical resolution parameters), whose variation provides a controlled estimate of systematic uncertainties associated with the truncation. Physical predictions are extracted from regions where the resulting masses exhibit maximal stability under such variations.

Finally, the robustness of the numerical results is assessed through:

- (i) convergence with respect to the number of radial and angular grid points, (N_q, N_z) ;
- (ii) stability under variations of the mapping scale Λ introduced in Eq. (41);
- (iii) independence of the extracted mass under changes of the ultraviolet cutoff;
- (iv) variation of the effective kernel strength to quantify truncation uncertainties;
- (v) propagation of uncertainties associated with the infrared RGZ parameters.

Together, these tests define a systematic uncertainty band for the extracted scalar glueball mass.

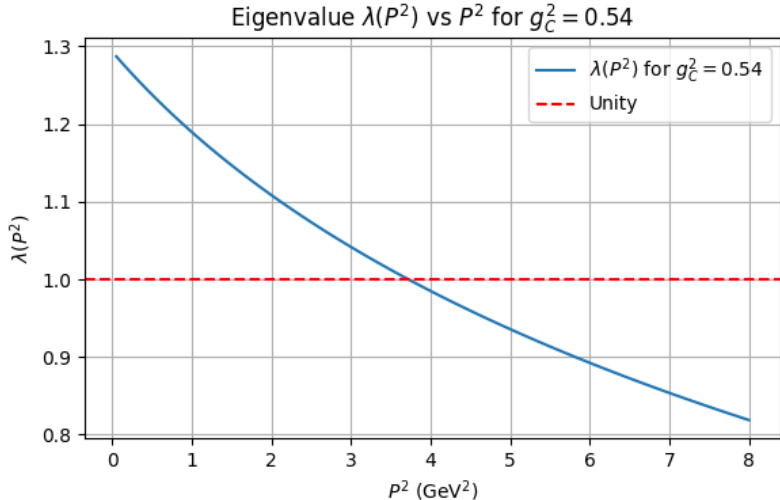


FIG. 1. Largest eigenvalue $\lambda(P^2)$ of the Bethe–Salpeter kernel as a function of P^2 for an effective coupling $g_C^2 = 0.54$. The intersection with the horizontal line $\lambda = 1$ fixes the scalar glueball mass.

VI. RESULTS AND COMPARISON WITH RGZ CORRELATOR APPROACHES

In this section we present the numerical solutions of the Euclidean BSE derived in the previous sections and compare the resulting scalar glueball mass with estimates obtained from correlator-based approaches within the RGZ framework.

At first sight, the numerical strategy adopted here differs from the correlator-based infrared moment analysis of Refs. [12, 20], which displays the glueball masses as functions of the subtraction scale T . This difference is, however, purely methodological. In the correlator approach, T is a non-physical parameter introduced by the subtraction procedure, and physical masses are extracted from regions of minimal sensitivity. In the present Euclidean Bethe–Salpeter formulation, an analogous role is played by the effective kernel strength g_C^2 , whose variation probes the truncation dependence of the bound-state equation. Although the graphical representations are different, both approaches rely on the same RGZ gluon propagator as infrared input and yield consistent scalar glueball mass estimates in the vicinity of 2 GeV.

To render the integral equation numerically tractable, we adopt a minimal truncation in which the Bethe–Salpeter kernel is approximated by an effective constant strength g_C^2 . In addition, we restrict ourselves to the dominant s -wave component of the amplitude by retaining only the lowest Chebyshev moment, $\Phi(p^2) \equiv \Phi_0(p^2)$, and neglecting its explicit angular dependence. Within these assumptions, the eigenvalue equation (37) reduces to a one-dimensional integral equation,

$$\lambda(P^2) \Phi(p^2) = g_C^2 \int_0^\infty dq^2 q^2 \int_{-1}^1 dz \mathcal{D}(q_+^2) \mathcal{D}(q_-^2) \Phi(q^2), \quad (45)$$

where the shifted momenta q_\pm^2 are given by Eq. (35) and the integration over relative angles has been reduced to a single variable z . The integrals are discretized on finite domains using Gauss–Legendre quadratures for both q^2 and z .

The gluon propagator $\mathcal{D}(p^2)$ entering Eq. (45) is the RGZ propagator given in Eq. (8), evaluated with representative parameter values motivated by lattice fits. In particular, Ref. [12] reports $m^2 + M^2 \simeq 0.34$ GeV 2 , $M^2 \simeq 2.15$ GeV 2 and $m^2 M^2 + 2g^2 N\gamma^4 \simeq 0.26$ GeV 4 . For the numerical analysis presented here we adopt the values $m^2 = 0.5$ GeV 2 , $M^2 = 2.0$ GeV 2 and $\lambda_4 = 0.26$ GeV 4 , which lie within the phenomenologically relevant window.

For fixed RGZ parameters, Eq. (45) is solved by varying the total momentum P^2 and determining the largest eigenvalue $\lambda(P^2)$. The bound-state condition corresponds to $\lambda(P^2) = 1$, with the scalar glueball mass given by $M_{0++}^2 = -P^2$. Since $\lambda(P^2)$ scales linearly with the effective coupling g_C^2 , one may equivalently view the procedure as tuning g_C^2 until a crossing occurs. Figure 1 shows a representative example of the eigenvalue $\lambda(P^2)$ as a function of P^2 for $g_C^2 = 0.54$. The eigenvalue decreases monotonically with increasing P^2 , and the crossing with $\lambda = 1$ unambiguously determines the bound-state mass.

TABLE I. Scalar glueball mass M_{0++} obtained from the simplified Euclidean Bethe–Salpeter equation for several values of the effective coupling g_C^2 . The RGZ parameters (m^2, M^2, λ_4) are kept fixed as described in the text.

g_C^2	M_{0++} (GeV)
0.50	1.55
0.52	1.75
0.54	1.93
0.56	2.10
0.58	2.26
0.60	2.41

The resulting scalar glueball masses obtained for several values of g_C^2 are listed in Table I. For couplings in the range $g_C^2 \simeq 0.52\text{--}0.58$, the extracted masses lie between approximately 1.7 and 2.3 GeV, with a preferred value close to $M_{0++} \simeq 1.9$ GeV around $g_C^2 \simeq 0.54$.

These values are in remarkable agreement with the scalar glueball mass obtained from RGZ correlator-based analyses. In particular, the infrared moment problem studied in Refs. [12, 20] yields an estimate $M_{0++} \approx 1.96$ GeV for SU(3), using the same RGZ gluon propagator as infrared input. In that approach, the two-point function of the gauge-invariant operator $\mathcal{O}_{0++} = \frac{1}{4}F_{\mu\nu}^a F_{\mu\nu}^a$ is expanded in infrared moments and analyzed via Padé approximants, with confinement encoded through the complex conjugate poles (“ i -particles”) of the RGZ propagator.

The present Bethe–Salpeter analysis offers a complementary perspective. While the correlator method directly probes the analytic structure of gauge-invariant two-point functions, the BSE framework interprets the scalar glueball as a bound state of infrared gluonic degrees of freedom and provides access to its Bethe–Salpeter amplitude. Despite the simplicity of the kernel employed here, both approaches lead to consistent mass estimates, underscoring the robustness of the RGZ description of infrared YM dynamics. A more refined treatment, including momentum-dependent kernels and higher Chebyshev moments, would allow for a quantitative assessment of systematic uncertainties and enable the extension of the present analysis to other glueball channels.

VII. CONCLUSIONS AND OUTLOOK

In this work we have formulated and numerically solved a Euclidean BSE for the lightest scalar glueball in pure YM theory, using the RGZ gluon propagator as an infrared-complete input. Within a minimal truncation characterized by an effective constant kernel strength and the dominant s -wave amplitude, we extracted scalar glueball masses in the range $M_{0++} \simeq 1.7\text{--}2.3$ GeV for representative values of the kernel parameter g_C^2 . A preferred value around 1.9 GeV was obtained for $g_C^2 \simeq 0.54$, in close agreement with correlator-based estimates within the RGZ framework [12, 20] and with contemporary lattice determinations. This concordance reinforces the robustness of the RGZ description of infrared gluodynamics and provides a nontrivial cross-check between bound-state and correlator approaches.

Our analysis showed that the BSE framework, even in a simplified truncation, is capable of capturing essential features of glueball dynamics when supplied with realistic nonperturbative propagators. We emphasized the conceptual correspondence between the effective kernel strength in the BSE and the subtraction-scale dependence encountered in infrared moment problems, showing that both play the role of nonphysical control parameters whose systematic variation quantifies truncation uncertainties. In this sense, the RGZ gluon propagator, with its complex conjugate poles encoding confinement, serves as a common infrared input across complementary methodologies.

Several directions for future investigations naturally emerge from the present study. First, the inclusion of momentum-dependent kernels and higher Chebyshev moments would allow for a more refined assessment of systematic uncertainties and may enable the resolution of excited glueball states. Such improvements would bring the present analysis closer to the level of sophistication achieved in meson and baryon studies within DSE/BSE frameworks.

A particularly promising avenue is the integration of our recent advances in physics-informed neural networks (PINNs) for solving DSEs [33, 34] into the present BSE approach. PINNs provide an efficient strategy for tackling nonlinear integral equations by embedding physical constraints directly into the learning architecture. Coupling PINN-based DSE solutions with a BSE treatment of glueball bound states could yield a powerful and flexible computational framework for exploring nonperturbative YM dynamics on multiple quantum-number channels. Another perspective is opened by our recent progress toward a unified formulation of gauge fixing in the presence of Gribov copies, interpolating between the ST and RGZ approaches [19]. By combining the present BSE program within such a unified gauge-fixing theory may give novel information into the interplay between gauge copies, infrared dynamics and bound-state formation.

Altogether, these developments point toward a comprehensive continuum approach to YM spectroscopy that harmonizes infrared analytic inputs, numerical bound-state techniques and modern computational tools. We believe that such an integrated program will significantly advance the understanding of pure gauge bound states and pave the way for future applications in full QCD.

[1] C. N. Yang and R. L. Mills. Conservation of isotopic spin and isotopic gauge invariance. *Phys. Rev.*, 96:191–195, 1954.

[2] L. D. Faddeev and V. N. Popov. Feynman diagrams for the yang–mills field. *Phys. Lett. B*, 25:29–30, 1967.

[3] V. N. Gribov. Quantization of nonabelian gauge theories. *Nucl. Phys. B*, 139:1–19, 1978.

[4] I. M. Singer. Some remarks on the gribov ambiguity. *Commun. Math. Phys.*, 60:7–12, 1978.

[5] A. Cucchieri and T. Mendes. Constraints on the ir behaviour of the gluon propagator in yang–mills theories. *Phys. Rev. Lett.*, 100:241601, 2008.

[6] I. L. Bogolubsky, E.-M. Ilgenfritz, M. Müller-Preussker, and A. Sternbeck. The landau gauge gluon and ghost propagators in 4d SU(3) lattice gauge theory: Further results. *Phys. Lett. B*, 676:69–73, 2009.

[7] P. Boucaud, J. P. Leroy, A. L. Yaouanc, J. Micheli, O. Pene, and J. Rodriguez-Quintero. The infrared behaviour of the pure Yang-Mills green functions. *Few Body Syst.*, 53:387–436, 2012.

[8] A. Maas. Describing gauge bosons at zero and finite temperature. *Phys. Rept.*, 524:203–300, 2013.

[9] D. Zwanziger. Local and renormalizable action from the gribov horizon. *Nucl. Phys. B*, 323:513–544, 1989.

[10] D. Zwanziger. Quantization of gauge fields, classical gauge invariance, and gluon confinement. *Nucl. Phys. B*, 345:461–482, 1990.

[11] D. Dudal, J. A. Gracey, S. P. Sorella, N. Vandersickel, and H. Verschelde. Refining the gribov–zwanziger approach in the landau gauge: Infrared propagators in harmony with the lattice results. *Phys. Rev. D*, 78:065047, 2008.

[12] D. Dudal, O. Oliveira, and N. Vandersickel. Indirect lattice evidence for the refined gribov–zwanziger formalism and the gluon condensate $\langle a^2 \rangle$ in the landau gauge. *Phys. Rev. D*, 81:074505, 2010.

[13] S. P. Sorella et al. Nonperturbative aspects of euclidean Yang–Mills theories in linear covariant gauges: Nielsen identities and a BRST-invariant two-point correlation function. *Phys. Rev. D*, 92:045039, 2015.

[14] S. P. Sorella et al. A local and BRST-invariant Yang–Mills theory within the gribov horizon. *Phys. Rev. D*, 95:045011, 2017.

[15] R. Carmo Terin et al. All-order renormalizable refined Gribov–Zwanziger model with BRST-invariant fermionic horizon function in linear covariant gauges. *Phys. Rev. D*, 104(5):054048, 2021.

[16] J. Serreau and M. Tissier. Lifting the gribov ambiguity in Yang–Mills theories. *Phys. Lett. B*, 712:97–103, 2012.

[17] J. Serreau, M. Tissier, and A. Tresmontant. Covariant gauges without gribov copies. *Phys. Rev. D*, 92:105003, 2015.

[18] U. Reinosa, J. Serreau, R. Carmo Terin, and M. Tissier. Symmetry restoration and the gluon mass in the landau gauge. *SciPost Phys.*, 10(2):035, 2021.

[19] Rodrigo Carmo Terin. Towards a unified viewpoint of gribov–zwanziger and serreau–tissier gauge fixing. 2025. arXiv preprint.

[20] D. Dudal, M. S. Guimaraes, and S. P. Sorella. Glueball masses from an infrared moment problem. *Phys. Rev. Lett.*, 106:062003, 2011.

[21] H. A. Bethe and E. E. Salpeter. A relativistic equation for bound-state problems. *Phys. Rev.*, 84:1232–1242, 1951.

[22] R. Alkofer and L. von Smekal. The infrared behavior of QCD Green's functions: Confinement, dynamical symmetry breaking, and hadrons as relativistic bound states. *Phys. Rept.*, 353:281–465, 2001.

[23] M. Q. Huber. Nonperturbative properties of Yang–Mills theories. *Phys. Rept.*, 879:1–92, 2020.

[24] J. M. Pawłowski. Aspects of the functional renormalisation group. *Annals Phys.*, 322:2831–2915, 2007.

[25] N. Nakanishi. *Graph Theory and Feynman Integrals*. Gordon and Breach, New York, 1971.

[26] J. Carbonell and V. A. Karmanov. Solving bethe–salpeter equation in minkowski space. *Eur. Phys. J. A*, 27:1–9, 2006.

[27] J. Carbonell and V. A. Karmanov. Solving bethe–salpeter equation for two fermions in minkowski space. *Eur. Phys. J. A*, 46:387–397, 2010.

[28] Wayne de Paula and Tobias Frederico. Minkowski space dynamics and light-front projection. 2026. arXiv preprint.

[29] J. Meyers and E. S. Swanson. Spin-zero glueballs in the Bethe–Salpeter formalism. *Phys. Rev. D*, 87(3):036009, 2013.

[30] H. Sanchis-Alepuz, R. Williams, R. Alkofer, and C. S. Fischer. On the gluon bound state spectrum in Yang–Mills theory. *Phys. Rev. D*, 92(3):034001, 2015.

[31] M. Q. Huber, C. S. Fischer, and H. Sanchis-Alepuz. Glueball properties from the Dyson–Schwinger/Bethe–Salpeter equations. *Eur. Phys. J. C*, 80(11):1077, 2020.

[32] A. C. Aguilar, A. A. Natale, and P. S. Rodrigues da Silva. Relating a gluon mass scale to an infrared fixed point in pure gauge qcd. *Phys. Rev. Lett.*, 90:152001, 2003.

[33] Rodrigo Carmo Terin. Physics-informed neural networks viewpoint for solving the dyson–schwinger equations of quantum electrodynamics. *SciPost Phys. Core*, 8:054, 2025.

[34] Rodrigo Carmo Terin. Spectral functions in minkowski quantum electrodynamics from neural reconstruction: Benchmarking against dispersive dyson–schwinger integral equations. *arXiv*, 2025.